THE JOURNAL OF BIOLOGICAL CHEMISTRY VOL. 290, NO. 21, pp. 13053–13063, May 22, 2015

Histone Chaperone HIRA in Regulation of Transcription Factor RUNX1*

Received for publication, September 30, 2014, and in revised form, March 31, 2015 Published, JBC Papers in Press, April 6, 2015, DOI 10.1074/jbc.M114.615492

Aditi Majumder[‡], Khaja Mohieddin Syed[‡1], Sunu Joseph[‡2], Peter J. Scambler[§3], and Debasree Dutta[‡4]

From the [‡]Cancer Research Program, Rajiv Gandhi Centre for Biotechnology, Thycaud PO, Poojappura, Thiruvananthapuram, 695 014 Kerala, India and the [§]Institute of Child Health, University College of London, London WC1E 6BT , United Kingdom

Background: RUNX1 is indispensable for endothelial to hematopoietic transition involving generation of hematopoietic stem cells from hemogenic endothelium.
Results: Histone chaperone HIRA interacts with RUNX1, incorporates H3.3 variant within enhancer element, and regulates downstream targets of RUNX1 implicated in definitive hematopoiesis.
Conclusion: HIRA regulates RUNX1.
Significance: A histone chaperone-transcription factor complex is implicated in hemogenic to hematopoietic transition.

RUNX1 (Runt-related transcription factor 1) is indispensable for the generation of hemogenic endothelium. However, the regulation of RUNX1 during this developmental process is poorly understood. We investigated the role of the histone chaperone HIRA (histone cell cycle regulation-defective homolog A) from this perspective and report that HIRA significantly contributes toward the regulation of RUNX1 in the transition of differentiating mouse embryonic stem cells from hemogenic to hematopoietic stage. Direct interaction of HIRA and RUNX1 activates the downstream targets of RUNX1 implicated in generation of hematopoietic stem cells. At the molecular level, HIRA-mediated incorporation of histone H3.3 variant within the *Runx1* +24 mouse conserved noncoding element is essential for the expression of *Runx1* during endothelial to hematopoietic transition. An inactive chromatin at the intronic enhancer of *Runx1* in absence of HIRA significantly repressed the transition of cells from hemogenic to hematopoietic fate. We expect that the HIRA-RUNX1 axis might open up a novel approach in understanding leukemogenesis in future.

Multipotent hematopoietic stem cells (HSCs)[5] arise during development and gradually colonize within liver, spleen, and finally bone marrow. Embryonic hematopoiesis encompasses two distinct processes of primitive and definitive hematopoiesis. Primitive hematopoiesis originates in the yolk sac at E7.25. In the case of definitive hematopoiesis, erythroid and myeloid progenitors are generated at E8.25 (1), and at E10.5 HSCs are detected in the aorta gonad mesonephros (AGM) region. Erythroid and myeloid progenitors are generated from a special subset of endothelial cells scattered within blood vessels called hemogenic endothelium (HE) (2, 3). HE undergoes endothelial to hematopoietic transition (EndHT) (4) to generate HSCs. EndHT is predominantly regulated by RUNX1 that belongs to the Runt-related transcription factor (RUNX) family of proteins. The RUNX1 knock-out embryos displayed a lack of fetal liver hematopoiesis (5) and died between E11.5 and E12.5 because of hemorrhaging in the central nervous system (6). Interestingly, RUNX1 can potentially modify the epigenetic status at the loci involved in hemogenic to hematopoietic transition (7). It can also physically interact with the histone methyltransferase to regulate hematopoiesis (8). However, the regulation of RUNX1 itself at the epigenetic level is poorly understood. Earlier, we demonstrated that HIRA-dependent histone H3.3 acetylation at lysine 56 residues could regulate the expression of endothelial specific genes (9). Functionally, HIRA acts to incorporate histone variant H3.3 into chromatin in a DNA replication-independent manner (10). The importance of HIRA during mammalian development is evident from the targeted mutagenesis study in mouse (11). HIRA null mice die between E10 and E11 and display a wide range of phenotypes secondary to defective mesendodermal development (11). Because RUNX1 is essential for the endothelial to hematopoietic transition, we were interested to investigate the potential role of histone chaperone HIRA in regulation of RUNX1 in endothelial to hematopoietic transition to HSCs.

Materials and Methods

Mouse Yolk Sac Study—E9.5 C57BL/6J mouse embryos were isolated along with the yolk sac. Yolk sacs were cleaned from the debris, fixed in 3.7% formaldehyde, and treated as described for the immunofluorescence study. Six yolk sac samples from two different pregnant mice were studied.

Culture of ES Cells—Mouse W9.5 (control) and *Hira*$^{-/-}$ ES cells (12) were cultured on a mitomycin C treated feeder layer for initial passages. For experiments, the cells were cultured in

* This work was supported by Grant SB/FT/LS-158/2012 from the Department of Science & Technology, India, and by intramural funding from the Department of Biotechnology, India.
[1] Supported by Fellowship DBT/JRF/13/AL/452 from the Department of Biotechnology (DBT), India.
[2] Supported by DBT Fellowship BT/PR5754/MED/31/167/2012.
[3] Supported by British Heart Foundation Grant RG/15/13/28570.
[4] To whom correspondence should be addressed: Cancer Research Program, Rajiv Gandhi Centre for Biotechnology, Thycaud PO, Poojappura, Thiruvananthapuram, 695 014 Kerala, India. Tel.: 4712529597; Fax: 4712348096; E-mail: debasreedutta@rgcb.res.in.
[5] The abbreviations used are: HSC, hematopoietic stem cell; ESC, embryonic stem cell; qRT-PCR, quantitative RT-PCR; EB, embryoid body; E*n*, embryonic day *n*; HE, hemogenic endothelium; EndHT, endothelial to hematopoietic transition.

TABLE 1
Primers for qRT-PCR analysis

Gene	Forward (5′ → 3′)	Reverse (3′ → 5′)
Hira	CAGGAGGATGACGAGAAGGA	ACTGTTTGACCACCGCACAC
Runx1	CCATAGAGCCATCAAAATCAC	GCTTGGTCTGATCATCTAGTTTC
Cmyb	GTCCTCTGTCTTCCCACAGG	TGTCCTCAAAGCCTTTACCG
Tie2	CTTAGTGACCATTCTCCCTCC	TGTCCAAGAAACCATAGCTG
Sox17	ACGCTAGCTCAGCGGTCTACTATT	AGGGATTTCCTTAGCGCTTCCAGG
Gata4	GAAAACGGAAGCCCAAGAAC	GGGAGGGTCTCACCAGCA
Nestin	TGTCCCTTAGTCTGGAAGTGG	GGTGTCTGCAAGCGAGAGTT
Gfi1	TCCGAGTTCGAGGACTTTTG	ACTGCCGATAGCTCTGCAC
Gata2	AAAGGGGCTGAATGTTTCG	GCGTGGGTAGGATGTGTC
Pu.1	GAGTTTGAGAACTTCCCTGAG	TGGTAGGTCATCTTCTTGCGG
Flk1	AATGGAGAAACAGAGCCACA	ATCCATAGGCGAGATCAAGG
Gfi1b	ATGGGGAATCACCACTCTCTG	GGGGTCTGTGTGTAGCTGT
Gapdh	TGCCCCCATGTTTGTGATG	TGTGGTCATGAGCCCTTCC
Runx1 (human)	CTGCTCCGTGCTGCCTAC	AGCCATCACAGTGACCAGAGT
Gata1 (human)	TGCTCTGGTGTCCTCCACAC	TGGGAGAGGAATAGGCTGCT
β-Actin (human)	CCAGCTCACCATGGATGATG	ATGCCGGAGCCGTTGTC

feeder-free conditions in ES medium composed of Iscove's modified Dulbecco's medium (Invitrogen; 12440053), 15% ES qualified serum (Invitrogen; 10439024), 1% antimycotic/antibiotic (Invitrogen; 15240062), 0.0124% 1-thioglycerol (Sigma; M6145), and 1% penicillin and streptomycin (Invitrogen; 10378016). We maintained them in undifferentiated condition by addition of 10^5 units of LIF/ml (Millipore; ESG1106) (13).

Embryoid Body (EB) Generation—3×10^5 control and *Hira*$^{-/-}$ ES cells were grown in ES medium for 2 days in feeder-free conditions before differentiation. To generate EBs, ES cells were grown in the absence of LIF in ES differentiation medium of Iscove's modified Dulbecco's medium containing 15% FCS selected for endothelial cell differentiation (Stem Cell Technologies; 06907), 1% ascorbic acid (5 mg/ml in 100 ml; Stem Cell Technologies; 07157), and 0.0124% 1-thioglycerol for 5 days (13).

ESC Differentiation to Hemogenic Endothelium and Hematopoietic Precursors—For the differentiation of HE from undifferentiated ES cells, we followed the protocol described by Chiang and Wong (14) with few modifications. Briefly, control and *Hira*$^{-/-}$ ES cells were cultured in serum- and feeder-free N2B27 medium (15) for 48 h. At day 2, 5 ng/ml BMP4 (R&D Systems; 314-BP-050), 4 ng/ml activin A (R&D Systems; 338-AC-010), 12.5 ng/ml FGF2 (R&D Systems; 233-FB-025), and 3 μM CHIR99021 (Stemgent; 130-095-555) were supplemented in the medium. At day 4, cells cultured in the presence of mesodermal inducer (mentioned above) were dissociated, sorted for FLK1$^+$ cells, and replated on 12-well plate at a concentration of 5×10^4 cells/well in N2B27 medium supplemented with 20 ng/ml BMP4, 12.5 ng/ml FGF2, 20 ng/ml VEGF165, 0.25 mM BrcAMP (Sigma; B5386), and 4 μM ALKi (Merck; 616461). At day 6, adherent cells and floating fractions were collected by trypsinization and trituration, respectively, for further study (14).

Culture of Kasumi-1 Cells—Kasumi-1 cells were cultured in RPMI medium (Himedia; AL1621) supplemented with 20% FBS, 1% antimycotic/antibiotic, and 1% penicillin and streptomycin.

Ectopic Expression of HIRA—Mouse *Hira* cDNA (accession number BC156807; MGC premier ORF clone TOM6004) purchased from TransOMICS Technologies was PCR-amplified and subcloned into pEGFP-C1 (Clontech; catalog number 6084-1) at XhoI and SalI sites.

Transfection—2×10^5 control and *Hira*$^{-/-}$ ES cells were seeded in Opti-MEM (Invitrogen; 31985088) on 12-well plates. Cells were transfected with Lipofectamine 2000 (Invitrogen; 11668019) and 2 μg of H3.3-Flag-tagged plasmid (Gift from Prof. James J. Bieker) and selected for 72 h with G418 (Sigma; G8168). In *Hira*$^{-/-}$ ES cells, HIRA was ectopically expressed by transfection of pEGFP-C1/*Hira* cDNA plasmid with Lipofectamine 2000. Transfected cells were observed for the expression of GFP and selected with G418 for 72 h.

Fluorescence-associated Cell Sorting—Control and *Hira*$^{-/-}$ ES cells were trypsinized and centrifuged at 1200 rpm for 5 min. Pellet was washed with FACS buffer (Dulbecco's phosphate-buffered saline with 0.8% (v/v) FBS and 0.263 mM EDTA (Sigma; E9884)) twice at 2000 rpm for 5 min. The cells were suspended in the FACS buffer and incubated with 0.5 μg of fluorescent-conjugated monoclonal antibody for 30 min in dark on ice. Following incubation, cells were centrifuged and resuspended in 500 μl of FACS buffer, filtered by cell strainer, and subsequently sorted by BD FACS Avia^{TM} II.

Quantitative RT-PCR—Total RNA from cells were extracted with TRIzol reagent (Invitrogen; 15596018); cDNA preparation was accomplished by a high capacity cDNA reverse transcription kit (ABI; 4368814), and the expression of genes were analyzed by qRT-PCR using Sybr Green master mix (ABI, #4367659). Primer sequences are listed in Table 1.

Western Blot—Protein concentrations were determined by the Bradford reagent (Bio-Rad) and resolved by 8 or 10% SDS-PAGE. Antibodies have been listed in Table 2.

Immunofluorescence and Confocal Microscopy—Immunostaining to detect expression of RUNX1 and HIRA in E9.5 yolk sacs, undifferentiated ES cells, and HE cells was performed using standard protocols. ESCs were cultured on coverslips under different culture conditions. Briefly, cells or yolk sacs were fixed with 3.7% paraformaldehyde (Sigma; P6148) and permeabilized with 0.2% Tween 20 (Sigma; P1379) in Dulbecco's phosphate-buffered saline (Invitrogen; 14190235). Nonspecific binding was blocked with 10% goat serum (Jackson Immunoresearch; 005-00-121), and cells were incubated overnight with primary antibody at a dilution of 1:200. Fluorescent conjugated secondary antibodies (Alexa Fluor 568; Invitrogen; A11004 and Alexa Flour 488; Invitrogen; A11008) were used at a 1:200 dilution. Coverslips were mounted on slides and observed using a confocal microscope. We used Hoechst dye

TABLE 2
Antibodies used in the study
IF, immunofluorescence; WB, Western blotting; BRG1, Brahma-related gene-1; PE, phycoerythrin.

	Company	Catalog number
Primary antibody		
RUNX1(WB; IP; IF)	Santa Cruz	sc-365644
RUNX1 (ChIP; IF)	Abcam	ab23980
HIRA (WB; IF)	Abcam	ab20655
β-Actin (EB)	Sigma	A5441
BRG1 (WB)	Santa Cruz	sc-10768
GATA2	Abcam	ab22849
FLAG (DDDDK)	Abcam	ab1162
FLK1	Cell Signaling	2479S
Histone H3	Cell Signaling	9715S
Secondary antibody		
Anti-mouse	Santa Cruz	sc-2005
Anti-rabbit	Santa Cruz	sc-2004
FACS antibody		
PE rat anti-mouse Flk1	BD Pharmingen	555308

(Sigma; #B1155, 1 μg/ml) for nuclear staining. For hematopoietic precursors, slides were coated with 0.1% poly-L-lysine (Sigma; 9813) for 30 min. Drops of cell culture suspension were added onto the slides and left for 4 h of incubation in a CO_2 incubator at 37 °C. Slides were further processed as described previously.

RNA Interference—Mouse *Hira* shRNA validated from our earlier study (9) was used to knockdown *Hira* in ES cells. Human *Hira* shRNAs were generated using iRNAi software. Lentiviral vectors containing shRNA targeting human *Hira* was cloned in the Plko.1 (Addgene) vector. Lentiviral supernatant was produced in HEK293T cells by transient transfection using calcium chloride (9). Briefly HEK293T cells were grown to 80% confluency. pRRE (gag/pol), pMD2G (VSVG), pRSV (Rev), and *Hira* shRNA plasmids were mixed in 0.25 M $CaCl_2$ and equilibrated with an equal volume of 2× HEPES-buffered saline. Lentiviral particle containing supernatants were collected after 24 h of incubation. ES cells or Kasumi-1 cells were grown to 70% confluence and transfected with lentiviral soups. Transfected cells were selected by the addition of 1 μg/ml of puromycin (Sigma, #P8833). After 3 days, RNA and protein were extracted for analysis. Quantitative RT-PCR and Western blotting confirmed the knockdown. We screened three different sets of shRNA, where sh247 (CCACAATGGCAAGCCGATT) worked best for the knockdown of *Hira* in Kasumi-1 cells.

Co-immunoprecipitation—Protein lysates were prepared in radio immunoprecipitation assay buffer (10 mM Tris-HCl, pH 7.6, 1% Triton X-100, 1% Nonidet P-40, 1% sodium deoxycholate, 0.1% SDS, 150 mM NaCl, 5 mM EDTA, 1 mM sodium orthovanadate, 1 mM PMSF, 10 mg/ml aprotinin) (16). Protein concentrations were determined by Bradford reagent (Bio-Rad). Lysates were immunoprecipitated with primary antibody. Immune complexes were adsorbed to protein A-Sepharose (Sigma; P3391) and resolved on 8% or 10% PAGE.

ChIP Analysis—Real time PCR-based quantitative ChIP analysis was performed as described previously (9, 13). Briefly, cells were trypsinized, cross-linked with formaldehyde (1%), and sonicated to generate chromatin fragments. Antibodies were used to immunoprecipitate protein-DNA cross-linked fragments. Precipitated complexes were eluted and reverse cross-linked. Enrichment of chromatin fragments was measured by qRT-PCR using Sybr Green fluorescence relative to a standard curve of input chromatin. Primer sequences are listed in the Tables 3 and 4.

Statistical Analysis—Student's two-tailed, unpaired *t* test was used to determine statistical significance. *p* values less than 0.05 were considered to be significant.

Results

HIRA Influence RUNX1 during Development—Establishment of hemogenic endothelium forms an integral part of development. At E9.5, mouse yolk sac expresses the key hemogenic marker RUNX1 in the circulation (17). To explore the function of HIRA in development, we utilized the classical embryonic stem cell (ESC) differentiation model for the formation of EBs. During differentiation, there is no significant change of *Hira* at the mRNA level (Fig. 1*A*), whereas Western blot analysis showed that protein expression was significantly increased (Fig. 1*B*). To assess the requirement for HIRA during differentiation, we generated EBs from $Hira^{-/-}$ ESCs. In concordance with an earlier report (18), we observed that the expression of the developmental genes *Gata4*, *Nestin*, and *Gata2* (Fig. 1, *C–E*) were induced in absence of HIRA. However, RUNX1 expression was significantly abrogated in absence of HIRA (Fig. 1*F*). This was confirmed by the down-regulation of RUNX1 protein in $Hira^{-/-}$ EBs (Fig. 1*G*). An analogous trend was observed in the *Tie2* mRNA level in EBs deprived of HIRA (Fig. 1*H*). Next, we examined the correlation between HIRA and RUNX1 protein expression during development in mouse, specifically within the yolk sac. Immunofluorescence study revealed that RUNX1 and HIRA co-localize in E9.5 mouse yolk sac (Fig. 1*I*).

HIRA Regulates RUNX1 in Hemogenic to Hematopoietic Transition—RUNX1 drives the generation of hemogenic endothelium and is required until the emergence of HSCs (4); on commitment to hematopoiesis, the role of RUNX1 becomes redundant. Because we demonstrated that RUNX1 expression is modulated by HIRA, we further investigated this relationship with regard to the hemogenic to hematopoietic transition. We generated HE from control and $Hira^{-/-}$ ESCs following the protocol described by Chiang and Wong (14). First, we questioned whether HIRA could influence the initial stages of differentiation of ESCs to HE. The differentiation in presence of mesodermal inducer and BMP4 induce the ESCs in endothelial lineage (14). Therefore, at day 4, we analyzed the expression of FLK1 (fetal liver kinase-1) in control and $Hira^{-/-}$ ES differentiated cells. $FLK1^+$ cells are common progenitors for endothelial and hematopoietic lineage. We observed that $Hira^{-/-}$ cells did not demonstrate any significant alteration in the expression of *Flk1* (Fig. 1, *J* and *K*). FACS analysis revealed a comparable number of $FLK1^+$ cells arising from both control and $Hira^{-/-}$ ESCs (Fig. 1*L*). Effectively, absence of HIRA could not inhibit or influence the differentiation of ESCs till the mesoderm stage. In the next stage, during hemogenic to hematopoietic transition, the phenotype of the cells undergoes a shift first from flattened to spherical cells and then from loosely bound cells to floating cells. Control ESCs conformed to this pattern of HE colony development (Fig. 2*A*, *upper panel*), whereas $Hira^{-/-}$ ESCs

TABLE 3
Primers for q-ChIP analysis
q-ChIP, quantitative ChIP.

Locus	Forward (5′ → 3′)	Reverse (3′ → 5′)
(−)14-kb *Pu.1*	CCTGGTTTCAGTCACTCCTCTGCT	TACTTCCTGCCTCCTCCCAGAAATC
(−)35-kb *Gfi1*	CCACATGACCTCATGAATGC	CCACAAACAGAACAGCTGGA
CNE3	CCAGCATGACACAGCAAATC	CCCAGGGCTTATCTGCAC
CNE2	GCTATTTCTGCCAAGGGTGA	GGGGTCTGAGGACCATGATA

TABLE 4
Primers of q-ChIP at *Runx1* +24/+25 mCNE locus
q-ChIP, quantitative ChIP.

Locus	Forward (5′ → 3′)	Reverse (3′ → 5′)
+24mCNE- L2	AAGTTCAGGCCACAGTGCTAGG	CTTCCATGCGGATCTTCACAG
+24mCNE- L2A	GCTTCAAACTCCCGTTCCTTCT	GGATGGGAGAGTGTGTGTGTGA
+24mCNE- L1A	CCACTGCACCTGCTAGGTTCTC	TCCCAGGCTCTTTGAGAAGAAA
+24mCNE″	GGGGCCCTCACTACCTCTTTTC	GGCTTCAACTGCCGGTTTATTT
+24mCNE′	ATGGTGTGAGGAGGAGACAGGA	ATGGTGTGAGGAGGAGACAGGA
+24mCNE- R1a	GCAGAGCTGATCAGAGGGTAGC	CAAGACCAGGGTCTGCAAGC
+24mCNE- R2d	CAGCAAATGGCATCTAAGACGTG	AACTTAGGTGTCAGGATCCAGAAGG

failed to generate colonies with an analogous morphology (Fig. 2*A*, *lower panel*). The *black arrows* in Fig. 2*A* (*upper panel*) indicate the small clusters of cells undergoing the classical EndHT. RUNX1 expression was significantly down-regulated at the protein level in hemogenic endothelial cells derived from *Hira*$^{-/-}$ ESCs (Fig. 2*B*). During the differentiation of ESCs toward HE, HSC precursors repopulate the floating fraction of the culture (14). Thus, we analyzed both the adherent cells and floating cells of the HE culture. In absence of HIRA, *Runx1* expression was significantly reduced in both the floating and adherent cells of the culture (Fig. 2*C*). We also analyzed the status of other genes associated with HE within the same samples. *Sox17* has been implicated in HE formation (19), and we observed that in HIRA depleted cells, there was no significant difference in its expression between the mutant and wild type HE cells (Fig. 2*D*). However, expression of c-*Myb*, a partner of RUNX1 (20) induced in hematopoietic differentiation (21), is significantly down-regulated within the *Hira*$^{-/-}$ HE (Fig. 2*D*). Endothelial marker *Tie2* was significantly down-regulated within the floating fraction of cells in the absence of HIRA (Fig. 2*D*). RUNX1 is a positive modulator of definitive hematopoiesis. Along with other transcription factors, RUNX1 regulates the dynamic pattern of genes implicated in hematopoiesis. *Pu.1*, *Gfi1*, and *Gfi1B* are reported to be direct downstream targets of RUNX1 (22, 23). Interestingly, the expression of the transcription factors *Pu.1*, *Gfi1*, and *Gfi1b* (Fig. 2*E*) were significantly down-regulated both in HE cells and hematopoietic precursors in the absence of HIRA. We conclude that HIRA is specifically involved in the regulation of RUNX1 during hemogenic program in the hemogenic-defined circuitry. Genes that are essential for hematopoietic progenitors are also affected as evident from the expression of *Gata2* (Fig. 2, *F* and *G*) or c-*myb* (Fig. 2*E*). On ectopic expression of HIRA (tagged with GFP) in *Hira*$^{-/-}$ ESCs (Fig. 3*A*, *left panels*), the expression of RUNX1 was rescued in differentiating HE cells (Fig. 3*A*, *right panel*).

To further understand the role of HIRA in the context of RUNX1 regulation, we studied the expression of RUNX1 in control and *Hira*$^{-/-}$ ESCs by immunofluorescence. Intriguingly, in absence of HIRA, we observed a lower intensity and altered localization of RUNX1 (Fig. 3*B*, *lower panel*) within the *Hira*$^{-/-}$ HE colony (Fig. 3*B*, lower panel) than within the control HE colony (Fig. 3*B*, *upper panel*). Interestingly, upon rescue by ectopic expression of HIRA, RUNX1 expression was induced with distinct localization within the nucleus (Fig. 3*C*). The hematopoietic precursors demonstrated intense RUNX1 and GATA2 co-localization in these rescued cells (Fig. 3*D*, *upper panel*), whereas the *Hira*$^{-/-}$ hematopoietic precursors displayed lowered and altered localization of RUNX1 (Fig. 3*D*, *lower panel*).

HIRA Level Linked to Nuclear Expression of RUNX1—What triggers the altered localization of RUNX1 in the hemogenic or hematopoietic clusters in absence of HIRA? To understand the mechanism for this altered or lesser nuclear expression of RUNX1 in the absence of HIRA, we generated a model of ESCs wherein we knocked down HIRA by shRNA expression (Fig. 4*A*). Interestingly, in a similar manner, EBs generated from *Hira*-kd ESCs showed significant down-regulation of *Runx1* (Fig. 4*B*) as observed in *Hira*$^{-/-}$ EBs (Fig. 1*F*). Immunofluorescence studies demonstrated that the intensity of RUNX1 was lowered in HE cells generated from *Hira*-kd ESCs (Fig. 4*C*). Effectively, few cells (indicated with *white arrows* in Fig. 4*C*, *lower panel*) appeared to have altered RUNX1 expression. Therefore, we infer that the reduced HIRA expression might be responsible for the inhibition of nuclear entry of the RUNX1, and hence an altered localization of RUNX1 in HE cells is observed.

HIRA Acts through RUNX1 to Modulate Definitive Hematopoiesis—Thus, we postulated that if depletion of HIRA reduces nuclear entry of RUNX1, then RUNX1 will be unable to bind to its targets and hematopoiesis will fail to initiate. We demonstrated that the expression of *Runx1* and its targets gets significantly down-regulated especially within the hematopoietic precursors (Fig. 2*E*). Further, RUNX1 binding to highly conserved and transcription factor rich binding regions at target loci is integral to the initiation of hematopoiesis. We therefore analyzed the region around (−)14 kb *Pu.1*, (−)35 kb *Gfi1*, and the enhancer elements CNE2 and CNE3 of *Gfi1b* by ChIP (7). RUNX1 has been reported to bind these regions and reshape the chromatin such that it becomes poised for hematopoiesis (7). Interestingly, ChIP analyses in HE cells showed

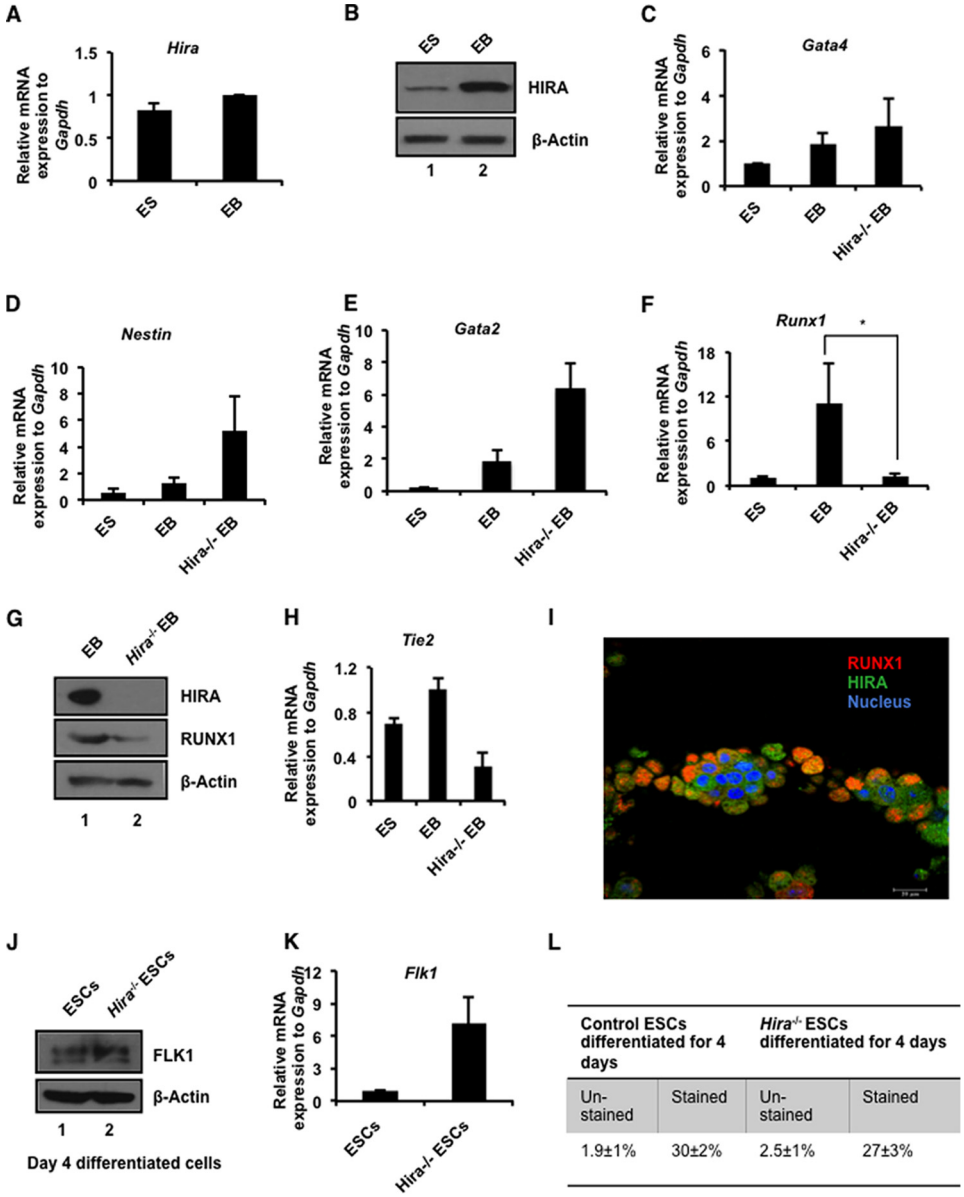

Control ESCs differentiated for 4 days		*Hira*$^{-/-}$ ESCs differentiated for 4 days	
Un-stained	Stained	Un-stained	Stained
1.9±1%	30±2%	2.5±1%	27±3%

FIGURE 1. **HIRA influence RUNX1 in development.** *A*, murine ES cells were differentiated into EBs in LIF free EB-specific medium and was subjected to RNA and protein isolation. Quantitative RT-PCR analysis of *Hira* in the ES-EB system (means ± S.E. for three independent experiments). *B*, the same sets of cells used in *A* were analyzed for the protein expression of HIRA by Western blot. *C–F*, control and *Hira*$^{-/-}$ ESCs were differentiated to EB formation. Quantitative RT-PCR analyses for different germ layer markers in ES/EB system (means ± S.E. for three independent experiments). *F*, the plot shows ($p < 0.05$) significant loss in expression of *Runx1* in *Hira*$^{-/-}$EB. *G*, Western blots for the same set of samples analyzed in *C–F*. *H*, quantitative RT-PCR analysis of *Tie2* in ES-EB system (means ± S.E. for three independent experiments). *I*, mouse yolk sac was isolated at E9.5 and immunostained for RUNX1 and HIRA expression. Magnification was 63× under oil immersion. *J*, control and *Hira*$^{-/-}$ ESCs were differentiated toward mesodermal lineage by mesoderm inducer growth factors for the generation of HE. Cells at day 4 were analyzed for the expression of FLK1 at protein level. *K*, same set of cells used in *J* was analyzed for the expression of *Flk1* at the mRNA level (means ± S.E. for three or more independent experiments). *L*, cells analyzed in *J* and *K* were sorted for FLK1 by FACS. The figure represents the fraction of FLK1^{+} control and *Hira*$^{-/-}$ cells. Averages of three independent experiments have been presented.

that, in the absence of HIRA, RUNX1 is not recruited at either the *Pu.1* and *Gfi1b* upstream regions or the enhancer elements of *Gfi1b* (Fig. 5, *A–D*). Analyses using EBs demonstrated a similar pattern of RUNX1 recruitment to target loci in the presence and absence of HIRA (Fig. 5, *A–D*). These data indicate HIRA could effectively regulate the RUNX1 targets in the context of HE and HSC generation. At the molecular level, HIRA and its associated complex (comprising ASF1, CAIN, and UBN1) physically interact with transcription factors, a chromatin insulator, and an ATP-dependent chromatin-remodeling complex (24). Therefore, we investigated whether HIRA and RUNX1 interacted within a protein complex. Co-immunoprecipitation experiments showed that RUNX1 physically associated with HIRA and vice versa (Fig. 6, *A* and *B*). The BRG1 component of the SWI-SNF chromatin remodeling complex has been implicated in regulating RUNX1 in the setting of leukemia and in the binding of the HIRA-complex to transcription factors (24, 25). Immunoprecipitation analyses demonstrated that BRG1 and RUNX1 interacted only in the presence of HIRA (Fig. 6*C*). Hence, the protein complex of HIRA, BRG1, and RUNX1 might

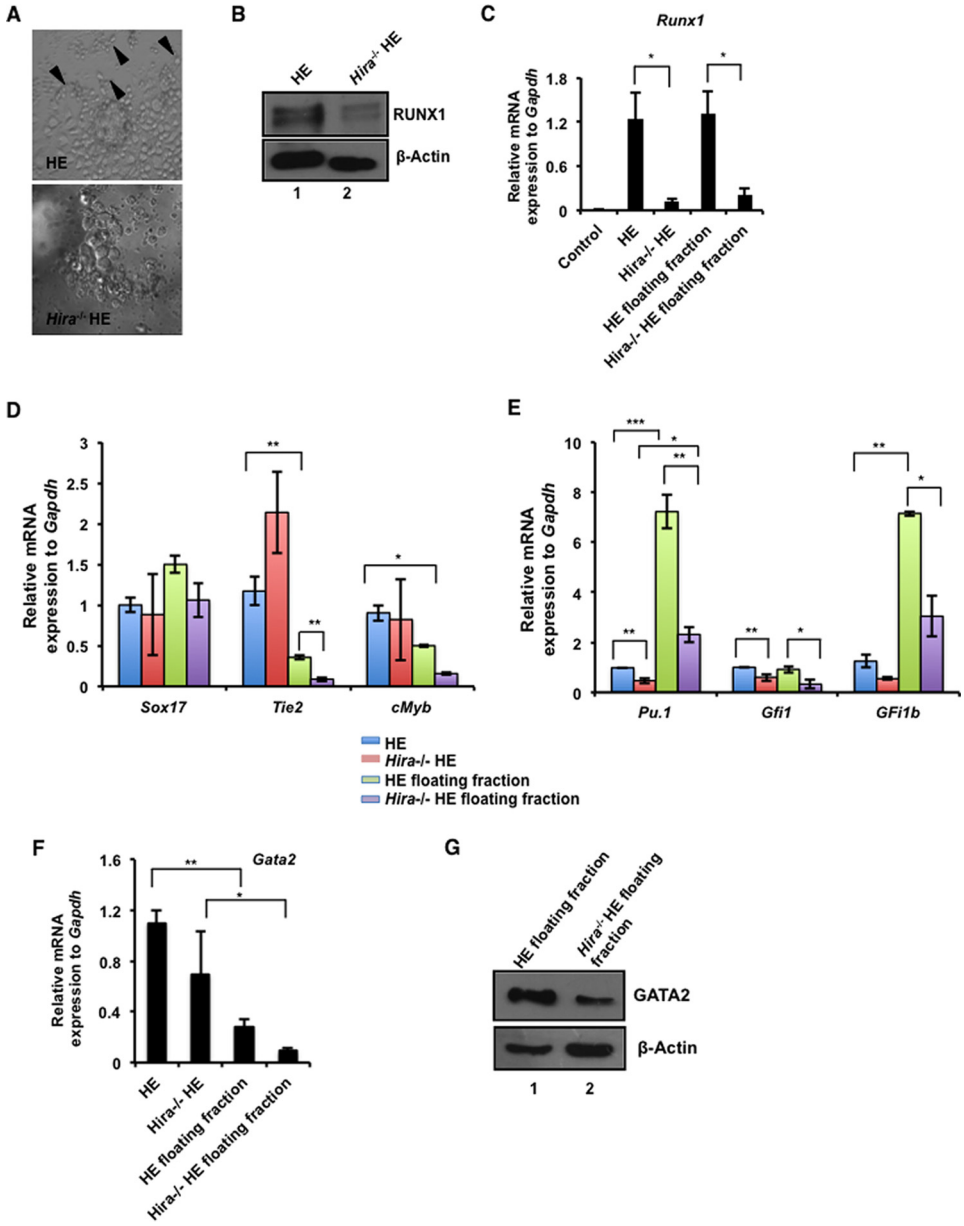

FIGURE 2. **HIRA regulates RUNX1 in endothelial to hematopoietic transition.** *A*, ES cells were differentiated toward hemogenic endothelium. Cells were cultured in serum-free medium for 48 h followed by culturing in the presence of BMP4, FGF2, GSKi, and Activin for the subsequent 48 h. Next, cells were allowed to differentiate in presence of VEGF, BrcAMP, BMP4, FGF2, or ALKi for 48 h to induce them toward HE. A phase contrast image of HE colony formed from control (*upper panel*) and *Hira*$^{-/-}$ ES cells (*lower panel*). The *black arrowheads* indicate the formation of typical round-shaped clusters of cells in control ES cells. These cells have undergone the EndHT. The representative clusters are absent in cells differentiated from *Hira*$^{-/-}$ ES cells. *B*, the above set of samples was analyzed for the presence of RUNX1 by Western blot. *C*, qRT-PCR analyses for the expression of *Runx*1 in the same set of samples including the floating fractions representing hematopoietic precursors (means ± S.E. for three independent experiments). *D*, quantitative RT-PCR analyses of other hemogenic and endothelial markers in the same samples analyzed in *C*. Statistical analyses indicate the significant change in the *Tie2* expression in adherent and floating fractions of control cells and within floating fractions of control and *Hira*$^{-/-}$ cells. Significant change was observed in c-*myb* expression in adherent and floating cells of control set. *E*, qRT-PCR analysis of RUNX1 target genes in hematopoiesis were analyzed in HE cells and hematopoietic precursors generated from control and *Hira*$^{-/-}$ ES cells (means ± S.E. for three independent experiments). Significant down-regulation of all the hematopoietic targets (*Pu.1*, *Gfi1*, and *Gfi1b*) of Runx1 is observed in the floating fractions of *Hira*$^{-/-}$ cells. *F*, quantitative RT-PCR analysis of *Gata2* in hematopoietic precursors and HE cells (means ± S.E. for three independent experiments). Significant down-regulation in *Gata2* expression within *Hira*$^{-/-}$ ESCs is observed. Statistical analyses were performed using Student's *t* test function. *, $p < 0.05$; **, $p < 0.01$; ***, $p < 0.001$. *G*, Western blot analysis for GATA2 expression in samples used in F.

subsequently modulate the expression of other hematopoietic genes targeted by RUNX1 within the nucleus.

HIRA-mediated H3.3 Enrichment within Runx1 Locus in Hemogenic to Hematopoietic Transition—Next, we asked how HIRA could regulate the expression of RUNX1 at the molecular level? Histone chaperone HIRA is responsible for the incorporation of Histone H3.3 variant in a replication-independent manner within the chromatin (10). Earlier reports indicate that a regulatory intronic enhancer termed as *Runx1* +24 mouse conserved noncoding elements (m CNE) is open and active for the expression of *Runx1* in cells undergoing hemogenic to hematopoietic transition (26). We determined the incorporation of Histone H3.3 variant within the enhancer region. We transfected control and *Hira*$^{-/-}$ ESCs with FLAG-tagged H3.3

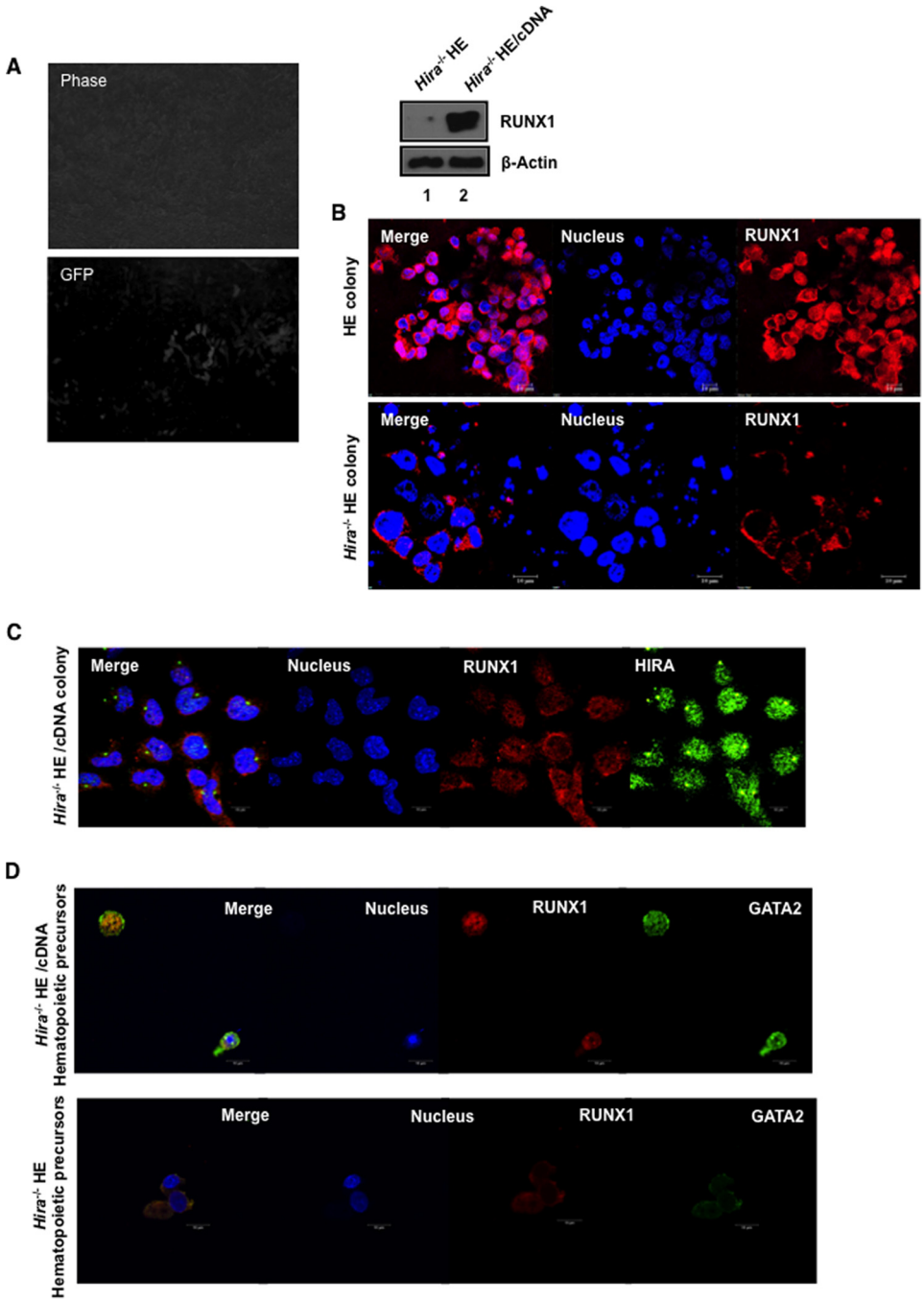

FIGURE 3. **HIRA rescues RUNX1 expression.** *A*, *Hira* (tagged to GFP) was ectopically expressed in $Hira^{-/-}$ ESCs (*left panel*) and differentiated to HE. Western blot analysis demonstrates the rescue of RUNX1 in the presence of HIRA (*right panel*). *B*, confocal study for the expression of RUNX1 within HE colonies generated from control and $Hira^{-/-}$ ESCs. *C*, localization of RUNX1 in $Hira^{-/-}$ HE cells with ectopic expression of HIRA. *D*, confocal study for the expression of RUNX1 and GATA2 in hematopoietic precursors of same set of cells analyzed in *C*.

construct (Fig. 6*D*) and differentiated them toward HE. We observed that H3.3 incorporation was significantly reduced in absence of HIRA within the enhancer region (Fig. 6*E*). We infer that HIRA-mediated histone H3.3 incorporation is required for the expression of *Runx1* during the hemogenic to hematopoietic transition.

Discussion

Histone chaperone HIRA mediated H3.3 acetylation at residue Lys-56 could regulate *in vitro* and *in vivo* model of angiogenesis by endothelial cells (9). Endothelial specific genes were down-regulated in HIRA knocked down yolk sac endothelial cells. Targeted mutagenesis of *Hira* led to abnormal mesendoderm development and disturbed gastrulation resulting in death of embryo *in utero* (11). To replicate a similar development pattern *in vitro*, we differentiated control and $Hira^{-/-}$ ES cells to form EBs. Expression of endodermal or ectodermal markers or genes implicated in early hematopoiesis were either induced or remained unaltered in EBs in absence of HIRA (Fig. 1). Earlier studies suggested

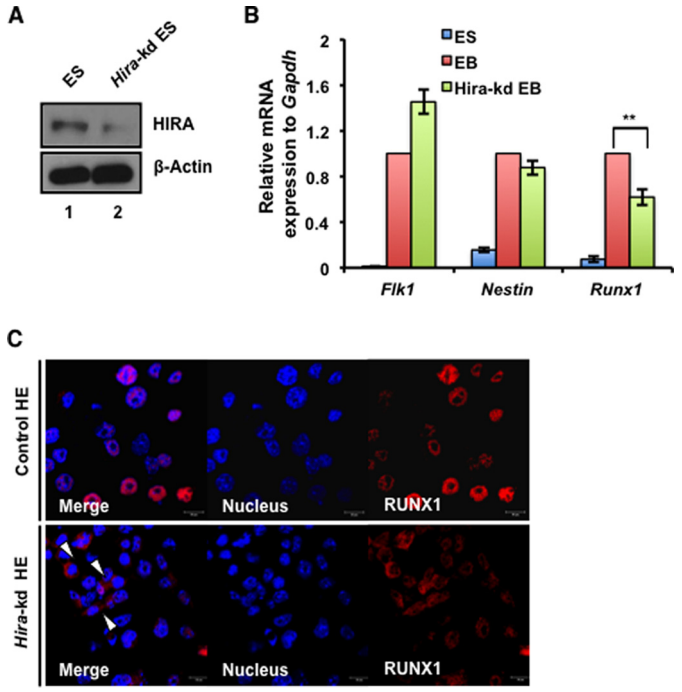

FIGURE 4. **Reduced level of HIRA associated with decreased and hence altered localization of RUNX1.** *A*, *Hira* was knocked down in control ESCs by shRNA expression. Western blot analysis demonstrates the knockdown of HIRA. *B*, EBs were generated from control and *Hira*-kd ESCs and analyzed for the expression of *Flk1*, *Runx1*, and *Nestin*. The expression of *Runx1* was significantly down-regulated in *Hira*-kd EBs. *C*, confocal study for the expression of RUNX1 in control and *Hira*-kd HE cells demonstrates differential localization of RUNX1. The *arrows* indicate cells showing altered RUNX1 localization. Statistical analyses were performed using Student's *t* test function. *, $p < 0.05$; **, $p < 0.01$; ***, $p < 0.001$.

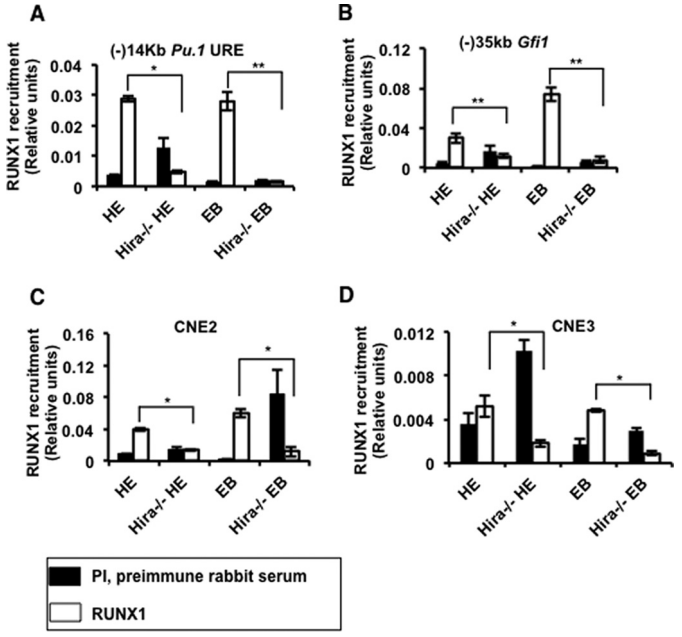

FIGURE 5. **HIRA in regulation of definitive hematopoiesis.** *A–D*, HE cells and EBs were generated from control and *Hira*$^{-/-}$ ES cells, cross-linked with 1% formaldehyde, and subjected to ChIP. The plots represent the recruitment of RUNX1 at the enhancer rich regions of *Pu.1* and *Gfi1* and at the enhancer elements (CNE3 and CNE2) of *Gfi1b* (means ± S.E. for three independent experiments). Preimmune rabbit serum (*PI*) is used as the negative control. Statistical analyses were performed using Student's *t* test function. *, $p < 0.05$; **, $p < 0.01$; ***, $p < 0.001$.

that the presence of unbound histones in *Hira*$^{-/-}$ EBs induces the expression of different germ layer markers (18). However, our data indicated that HIRA might have a differential regulatory role that could modulate the expression of RUNX1 during development.

These observations shaped the basis of determining the role of *Hira* in regulation of endothelial to hematopoietic transition. RUNX1 is essential for this particular cellular transition. Hence, we analyzed the HE colonies generated from control and *Hira*$^{-/-}$ cells and their subsequent transition to hematopoietic precursors. However, HIRA did not regulate the differentiation of ESCs toward the mesoderm because FLK1 expression remained unchanged in *Hira*$^{-/-}$ cells. It can be recalled here that up-regulation of FLK1 has been associated with down-regulation of RUNX1 in endothelial cells (27). Also, in our earlier studies we showed that expression of *Flk1* in response to angiogenic signals was independent of HIRA in endothelial cells (9). In the differentiation protocol adopted in this study, inclusion of BMP4 in the culture media and the sequential differentiation from ES cells eventually allow a higher yield of ~80% for both endothelial cells and blood or hematopoietic precursors (14) without the use of sorting processes between differentiation steps. We observed that on down-regulation of RUNX1 expression, the formation of specific morphological pattern of colonies of cells experiencing the EndHT was eventually distorted (Fig. 2*A*). Intriguingly, the absence of HIRA altered the subcellular localization of RUNX1 in HE cells (Fig. 3*B*). However, we demonstrated that the lower expression of *Hira* eventually led to the nonaccumulation or localization of nuclear RUNX1 (Fig. 4).

Understandably, nonavailability of RUNX1 within the nucleus affected its downstream targets especially those involved in definitive hematopoiesis. Other nontargets genes like c-*myb* were also affected in the hematopoietic precursors. We reasoned that a decrease in the level of hematopoietic specific markers is quite natural when the transition to hematopoiesis is hindered. Recently, Soni *et al.* (28) reported that *Hira* is critical for β-globin expression and few erythropoietic regulators but not the early hematopoietic marker *Gata2* in EBs. Our analyses in EBs demonstrated a similar result in respect to *Gata2* (Fig. 1*E*), but in the context of generation of hematopoietic precursors from *Hira*$^{-/-}$ HE cells, *Gata2* was significantly down-regulated in the hematopoietic precursors (Fig. 2*F*) and in HE cells at the mRNA level (Fig. 2*F*). We inferred that HIRA could regulate RUNX1 and its targets during EndHT. To understand the transcription factor and histone chaperone interaction, it should be noted that the HIRA complex of UBN1, CAIN, and ASF1 with chromatin modulators BRG1/INI1 could regulate the chromatin landscape on the basis of gene transcription (24). Interaction studies indicated that *Hira* is essential for the formation of the protein complex formed of RUNX1 and BRG1 to bind to other downstream targets of RUNX1.

EndHT followed by hematopoietic stem cell differentiation are structured by different sets of transcription factors including RUNX1. *Gfi1*, *Gfi1b*, and *Pu.1* have been implicated as direct targets of RUNX1 to establish the downstream hierarchy of hematopoiesis (23, 7, 29). The upstream region of myeloid master regulator *Pu.1* has more than one functionally essential

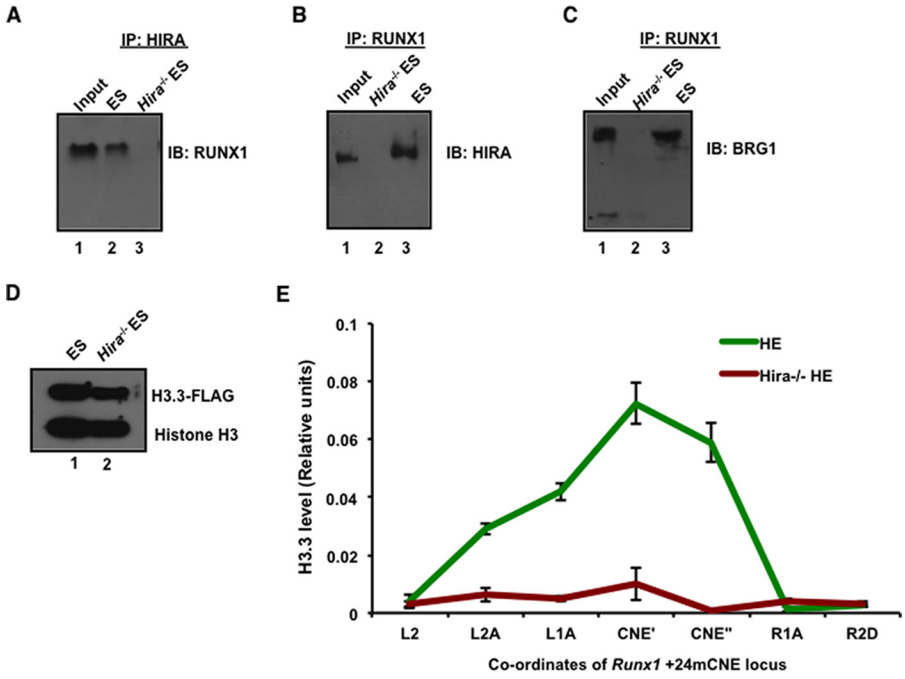

FIGURE 6. **HIRA-mediated incorporation of histone H3.3 variant within *Runx1* intronic enhancer drives hemogenic to hematopoietic transition.** *A* and *B*, co-immunoprecipitation of HIRA and RUNX1 in control and *Hira*$^{-/-}$ ESCs. Shown are results of immunoprecipitation (*IP*) with HIRA and immunoblot (*IB*) with RUNX1 and vice versa, wherein input is 14%. *C*, co-immunoprecipitation of RUNX1 and BRG1 in control and *Hira*$^{-/-}$ ESCs. Shown are results of immunoprecipitation with RUNX1 and immunoblot with BRG1, wherein input is 14%. *D*, H3.3-Flag-tagged plasmid was transfected in ESCs by Lipofectamine and selected with G418 for 72 h. Western blot for FLAG-H3.3 in control and *Hira*$^{-/-}$ ESCs. *E*, HE cells were generated from transfected control and *Hira*$^{-/-}$ ESCs, cross-linked with 1% formaldehyde, and subjected to ChIP. A 3.6-kb locus flanking +24mCNE (conserved noncoding elements) region was analyzed to determine the extent of H3.3 incorporation. The plot shows the reduced or loss in incorporation of H3.3 in *Hira*$^{-/-}$ HE cells within +24mouse conserved noncoding elements (*CNE*) implicated in hemogenic to hematopoietic transition. *PI* is preimmune rabbit serum, used as negative control. Statistical analyses were performed using Student's *t* test function. *, $p < 0.05$; **, $p < 0.01$; ***, $p < 0.001$.

RUNX1 binding sites (29). Similarly, upstream region and enhancer elements of *Gfi1* and *Gfi1b* have putative RUNX1 binding sites associated with definitive hematopoiesis (23). We demonstrated that reduced expression of RUNX1 in the nucleus within the cells deprived of HIRA could neither induce nor bind to the targets and hence could not establish the global reorganization at the chromatin level needed for the proper initiation of hematopoiesis (7), but how HIRA could influence the RUNX1 expression is the major concern of the study. Therefore, we explored the *cis*-regulatory elements of *Runx1*, essential for its expression during the transition. Ng *et al.* (26) reported that the *Runx1* +24 mCNE was specifically active in HE cells and sites associated with HSC generation. We observed that the region spanning ~3.6 kb has significant enrichment of H3.3 in control HE cells. We concluded that H3.3 incorporation by HIRA is essential to retain an active state of the enhancer element of *Runx1*.

Considering the fact that even in the complete absence of HIRA, there is always a constitutive expression of RUNX1, as evident from figures included in the study. There are few factors that might contribute to this level of expression of RUNX1. First, histone chaperone DAXX can occasionally complement the role of HIRA (30). Second, the incorporation of H3.3 is not completely abolished at the intronic *Runx1* enhancer (Fig. 6*E*). Therefore, we predict that few other aspects might contribute toward the regulation of RUNX1.

The transcription factor RUNX1 is also known as acute myeloid leukemia 1 protein or AML1. RUNX1 has been implicated in different types of leukemia in the context of chromosomal translocation or point mutation within this gene (31). Recent findings revealed that altered subnuclear localization of RUNX1 can switch cancer cells between proliferation and differentiation (32). Other histone chaperones including *Asf1b* and *Caf1p60* have been implicated in cancer (33–35), but how *Hira* could modulate different genes in the context of cancer has never been addressed. Based on our initial observation of HIRA-mediated regulation of RUNX1 in hematopoiesis, we considered whether this phenomenon could be relevant in leukemia cells. Our preliminary findings in leukemia cell line harboring AML1/ETO fusion revealed that on knockdown of HIRA in Kasumi cells (gift from Dr. O. Williams; Fig. 7*B*), a reduced expression of RUNX1 was observed (Fig. 7*C*). Interestingly, a significant gain in the expression of *Gata1* was detected at the RNA level (Fig. 7*C*). *Gata1* and other *Gata* factors are repressed under the influence of AML1/ETO and hence are responsible for the blockade of cells toward erythroid and megakaryocytic lineage (36). We anticipate that HIRA-mediated regulation of RUNX1 followed by induction in GATA1 level might shift the balance from proliferative to differentiation of leukemia cells. In summary, we report for the first time that the regulation of the transcription factor RUNX1 by histone chaperone HIRA operates within the murine hemogenic endothelium, and this pathway subsequently regulates genes expressed in HSCs and thus regulates the endothelial to hematopoietic transition (Fig. 7).

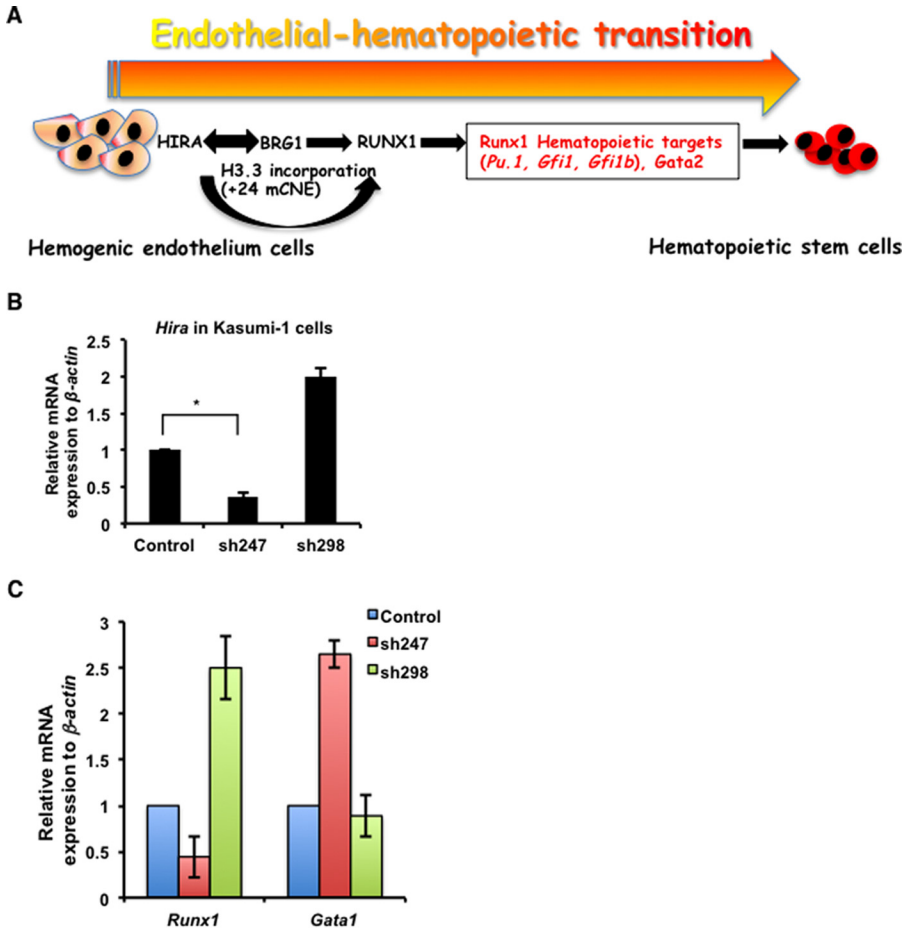

FIGURE 7. **HIRA regulates RUNX1.** *A*, summary of the proposed mechanism represent that HIRA interacting with the chromatin remodeler BRG1 regulates RUNX1 in EndHT and further contributes toward the regulation of hematopoietic targets of RUNX1 in generation of HSCs. *B*, Kasumi-1 cells harboring the t(8;21) translocation were analyzed for the HIRA-RUNX1 axis in leukemia. Quantitative RT-PCR analysis of *Hira* knockdown in Kasumi-1 cells. *C*, the same cells were analyzed for the expression of *Runx1* and *Gata1* by qRT-PCR. Control is unmanipulated Kasumi-1 cells. Statistical analyses were performed using Student's *t* test function. *, $p < 0.05$; **, $p < 0.01$; ***, $p < 0.001$.

Acknowledgments—We thank Prof. James Bieker, Dr. Owen Williams, and Dr. Arumugam Rajavelu for sharing reagents. We acknowledge the technical facilities at the host institute. The corresponding author also acknowledges the support of Dr. Ananda Mukherjee for providing critical comments on the manuscript.

Note Added in Proof—Khaja Mohieddin Syed's name was listed incorrectly in the version of the article that was published as a Paper in Press on April 6, 2015.

References

1. Palis, J., Robertson, S., Kennedy, M., Wall, C., and Keller, G. (1999) Development of erythroid and myeloid progenitors in the yolk sac and embryo proper of the mouse. *Development* **126,** 5073–5084
2. Bertrand, J. Y., Chi, N. C., Santoso, B., Teng, S., Stainier, D. Y., and Traver, D. (2010) Haematopoietic stem cells derive directly from aortic endothelium during development. *Nature* **464,** 108–111
3. Boisset, J. C., van Cappellen, W., Andrieu-Soler, C., Galjart, N., Dzierzak, E., and Robin, C. (2010) *In vivo* imaging of haematopoietic cells emerging from the mouse aortic endothelium. *Nature* **464,** 116–120
4. Chen, M. J., Yokomizo, T., Zeigler, B. M., Dzierzak, E., and Speck, N. A. (2009) Runx1 is required for the endothelial to haematopoietic cell transition but not thereafter. *Nature* **457,** 887–891
5. Okuda, T., van Deursen, J., Hiebert, S. W., Grosveld, G., and Downing, J. R. (1996) AML1, the target of multiple chromosomal translocations in human leukemia, is essential for normal fetal liver hematopoiesis. *Cell* **84,** 321–330
6. Wang, Q., Stacy, T., Binder, M., Marin-Padilla, M., Sharpe, A. H., and Speck, N. A. (1996) Disruption of the Cbfa2 gene causes necrosis and hemorrhaging in the central nervous system and blocks definitive hematopoiesis. *Proc. Natl. Acad. Sci.* **93,** 3444–3449
7. Lichtinger, M., Ingram, R., Hannah, R., Müller, D., Clarke, D., Assi, S. A., Lie-A-Ling, M., Noailles, L., Vijayabaskar, M. S., Wu, M., Tenen, D. G., Westhead, D. R., Kouskoff, V., Lacaud, G., Göttgens, B., and Bonifer, C. (2012)) RUNX1 reshapes the epigenetic landscape at the onset of haematopoiesis. *EMBO J.* **31,** 4318–4333
8. Koh, C. P., Wang, C. Q., Ng, C. E., Ito, Y., Araki, M., Tergaonkar, V., Huang, G., and Osato, M. (2013) RUNX1 meets MLL: epigenetic regulation of hematopoiesis by two leukemia genes. *Leukemia* **27,** 1793–1802
9. Dutta, D., Ray, S., Home, P., Saha, B., Wang, S., Sheibani, N., Tawfik, O., Cheng, N., and Paul, S. (2010) Regulation of angiogenesis by histone chaperone HIRA-mediated incorporation of lysine 56-acetylated histone H3.3 at chromatin domains of endothelial genes. *J. Biol. Chem.* **285,** 41567–41577
10. Green, E. M., Antczak, A. J., Bailey, A. O., Franco, A. A., Wu, K. J., Yates, J. R., 3rd, and Kaufman, P. D. (2005) Replication-independent histone deposition by the HIR complex and Asf1. *Curr. Biol.* **15,** 2044–2049
11. Roberts, C., Sutherland, H. F., Farmer, H., Kimber, W., Halford, S., Carey, A., Brickman, J. M., Wynshaw-Boris, A., and Scambler, P. J. (2002) Targeted mutagenesis of the Hira gene results in gastrulation defects and patterning abnormalities of mesoendodermal derivatives prior to early embryonic lethality. *Mol. Cell. Biol.* **22,** 2318–2328

12. Goldberg, A. D., Banaszynski, L. A., Noh, K. M., Lewis, P. W., Elsaesser, S. J., Stadler, S., Dewell, S., Law, M., Guo, X., Li, X., Wen, D., Chapgier, A., DeKelver, R. C., Miller, J. C., Lee, Y. L., Boydston, E. A., Holmes, M. C., Gregory, P. D., Greally, J. M., Rafii, S., Yang, C., Scambler, P. J., Garrick, D., Gibbons, R. J., Higgs, D. R., Cristea, I. M., Urnov, F. D., Zheng, D., and Allis, C. D. (2010) Distinct factors control histone variant H3.3 localization at specific genomic regions. *Cell* **140,** 678–691
13. Dutta, D., Ray, S., Home, P., Larson, M., Wolfe, M. W., and Paul, S. (2011) Self-renewal versus lineage commitment of embryonic stem cells: protein kinase C signaling shifts the balance. *Stem Cells* **29,** 618–628
14. Chiang, P. M., and Wong, P. C. (2011) Differentiation of an embryonic stem cell to hemogenic endothelium by defined factors essential role of bone morphogenetic protein 4. *Development* **138,** 2833–2843
15. Ying, Q. L., Wray, J., Nichols, J., Batlle-Morera, L., Doble, B., Woodgett, J., Cohen, P., and Smith, A. (2008) The ground state of embryonic stem cell self-renewal. *Nature* **453,** 519–523
16. Ray, S., Dutta, D., Rumi, M. A., Kent, L. N., Soares, M. J., and Paul, S. (2009) Context-dependent function of regulatory elements and a switch in chromatin occupancy between GATA3 and GATA2 regulate Gata2 transcription during trophoblast differentiation. *J. Biol. Chem.* **284,** 4978–4988
17. Samokhvalov, I. M., Samokhvalova, N. I., and Nishikawa, S. (2007) Cell tracing shows the contribution of the yolk sac to adult haematopoiesis. *Nature* **446,** 1056–1061
18. Meshorer, E., Yellajoshula, D., George, E., Scambler, P. J., Brown, D. T., and Misteli, T. (2006) Hyperdynamic plasticity of chromatin proteins in pluripotent embryonic stem cells. *Dev. Cell* **10,** 105–116
19. Clarke, R. L., Yzaguirre, A. D., Yashiro-Ohtani, Y., Bondue, A., Blanpain, C., Pear, W. S., Speck, N. A., and Keller, G. (2013) The expression of Sox17 identifies and regulates haemogenic endothelium. *Nat. Cell Biol.* **15,** 502–510
20. Hernandez-Munain, C., and Krangel, M. S. (1994) Regulation of the T-cell receptor delta enhancer by functional cooperation between c-Myb and core-binding factors. *Mol. Cell. Biol.* **14,** 473–483
21. Soza-Ried, C., Hess, I., Netuschil, N., Schorpp, M., and Boehm, T. (2010) Essential role of c-myb in definitive hematopoiesis is evolutionarily conserved. *Proc. Natl. Acad. Sci. U.S.A.* **107,** 17304–17308
22. Jin, H., Li, L., Xu, J., Zhen, F., Zhu, L., Liu, P. P., Zhang, M., Zhang, W., and Wen, Z. (2012) Runx1 regulates embryonic myeloid fate choice in zebrafish through a negative feedback loop inhibiting Pu.1expression. *Blood* **119,** 5239–5249
23. Lancrin, C., Mazan, M., Stefanska, M., Patel, R., Lichtinger, M., Costa, G., Vargel, O., Wilson, N. K., Möröy, T., Bonifer, C., Göttgens, B., Kouskoff, V., and Lacaud, G. (2012) GFI1 and GFI1B control the loss of endothelial identity of hemogenic endothelium during hematopoietic commitment. *Blood* **120,** 314–322
24. Pchelintsev, N. A., McBryan, T., Rai, T. S., van Tuyn, J., Ray-Gallet, D., Almouzni, G., and Adams, P. D. (2013) Placing the HIRA histone chaperone complex in the chromatin landscape. *Cell Rep.* **3,** 1012–1019
25. Bakshi, R., Hassan, M. Q., Pratap, J., Lian, J. B., Montecino, M. A., van Wijnen, A. J., Stein, J. L., Imbalzano, A. N., and Stein, G. S. (2010) The human SWI/SNF complex associates with RUNX1 to control transcription of hematopoietic target genes. *J. Cell. Physiol.* **225,** 569–576
26. Ng, C. E., Yokomizo, T., Yamashita, N., Cirovic, B., Jin, H., Wen, Z., Ito, Y., and Osato, M. (2010) A Runx1 intronic enhancer marks hemogenic endothelial cells and hematopoietic stem cells. *Stem Cells* **28,** 1869–1881
27. Hirai, H., Samokhvalov, I. M., Fujimoto, T., Nishikawa, S., Imanishi, J., and Nishikawa, S. (2005) Involvement of Runx1 in the down-regulation of fetal liver kinase-1 expression during transition of endothelial cells to hematopoietic cells. *Blood* **106,** 1948–1955
28. Soni, S., Pchelintsev, N., Adams, P. D., and Bieker J. J. (2014) Transcription factor EKLF (KLF1) recruitment of the histone chaperone HIRA is essential for β-globin gene expression. *Proc. Natl. Acad. Sci. U.S.A.* **111,** 13337–13342
29. Hoogenkamp, M., Krysinska, H., Ingram, R., Huang, G., Barlow, R., Clarke, D., Ebralidze, A., Zhang, P., Tagoh, H., Cockerill, P. N., Tenen, D. G., and Bonifer, C. (2007) The Pu.1 locus is differentially regulated at the level of chromatin structure and noncoding transcription by alternate mechanisms at distinct developmental stages of hematopoiesis. *Mol. Cell. Biol.* **27,** 7425–7438
30. Drané, P., Ouararhni, K., Depaux, A., Shuaib, M., and Hamiche, A. (2010) The death-associated protein DAXX is a novel histone chaperone involved in the replication-independent deposition of H3.3. *Genes Dev.* **24,** 1253–1265
31. Osato, M. (2004) Point mutations in the RUNX1/AML1 gene: another actor in RUNX leukemia. *Oncogene* **23,** 4284–4296
32. Zaidi, S. K., Dowdy, C. R., van Wijnen, A. J., Lian, J. B., Raza, A., Stein, J. L., Croce, C. M., and Stein, G. S. (2009) Altered Runx1 subnuclear targeting enhances myeloid cell proliferation and blocks differentiation by activating a miR-24/MKP-7/MAP kinase network. *Cancer Res.* **69,** 8249–8255
33. Corpet, A., De Koning, L., Toedling, J., Savignoni, A., Berger, F., Lemaître, C., O'Sullivan, R. J., Karlseder, J., Barillot, E., Asselain, B., Sastre-Garau, X., and Almouzni, G. (2011) Asf1b, the necessary Asf1 isoform for proliferation, is predictive of outcome in breast cancer. *EMBO J.* **30,** 480–493
34. Staibano, S., Mascolo, M., Mancini, F. P., Kisslinger, A., Salvatore, G., Di Benedetto, M., Chieffi, P., Altieri, V., Prezioso, D., Ilardi, G., De Rosa, G., and Tramontano, D. (2009) Overexpression of chromatin assembly factor-1 (CAF-1) p60 is predictive of adverse behaviour of prostatic cancer. *Histopathology* **54,** 580–589
35. Burgess, R. J., and Zhang, Z. (2013) Histone chaperones in nucleosome assembly and human disease. *Nat. Struct. Mol. Biol.* **20,** 14–22
36. Elagib, K. E., Racke, F. K., Mogass, M., Khetawat, R., Delehanty, L. L., and Goldfarb, A. N. (2003) RUNX1 and GATA-1 coexpression and cooperation in megakaryocytic differentiation. *Blood* **101,** 4333–4341